Factors affecting the nascent structure and morphology of polyethylene obtained by heterogeneous Ziegler–Natta catalysts: 1. Polymerization kinetics

A. Muñoz-Escalona and A. Parada
Laboratorio de Polimeros, Centro de Quimica, Instituto Venezolano de Investigaciones Cientificas IVIC, Apartado 1827, Caracas, Venezuela
(Received 4 April 1978; revised 28 November 1978)

Kinetic measurements were carried out to study the influence of polymerization conditions on the morphology and macroconformation of nascent polyethylene obtained with a heterogeneous $TiCl_3$/$Al(C_2H_5)_3$ Ziegler–Natta catalyst. The polymerization of ethylene in a n-paraffin viscous medium was studied for very different conditions, such as polymerization temperature from 0° to 120°C, pressures of 1 and 10 atm and stirring speed of 10 and 1000 r.p.m. It was established by electron microscopy that new polymer chains originate due to formation of new surfaces by break-up of catalyst aggregates and also through crystal scission. The average size of polymer globules growing on the catalyst surface was of the order of $10^8 cm^{-2}$. The same kinetic relationships are approximately obeyed when the polymerization is controlled by mass transfer of the monomer. The overall activation energies for the maximum polymerization rate, decay period and the stationary polymerization rate were: 8.4, 3.4 and 5.0 kcal/mol, respectively. Molecular weight measurements combined with polymerization rate determinations lead to the conclusion that the number of growing polymer chains increases with the polymerization temperature, being of the order of $10^{12} cm^{-2}$ at low temperature. This corresponds to a concentration of active sites of about 10^4 per polymerization locus.

INTRODUCTION

The morphology and structure of polymers crystallizing from the solution and melt has been extensively investigated[1–5]. The results have helped to understand the mechanical and technological properties of moulded end-products[6,7]. However, there are relatively few reports dealing with the morphology and structure of the as-polymerized materials[8,9]. From both the academic and technological point of view there is an interest in the furtherance of these studies. On the one hand, the achievements already made contribute to a wider knowledge of the process involved in crystallization of polymers[10]; on the other hand, the understanding of the factors controlling the morphology and structure of the polymers formed during polymerization are very important in the attempts to reduce cost in polymer processing by direct fabrication of finished, moulded products from the monomer (fibre, sheet)[11,12]. Finally, it has been established that from the morphology and macroconformation of the nascent polymers, conclusions can be obtained on how the polymerization takes place[13–17]. These considerations were all taken into account in our studies of the polymerization of ethylene using the $TiCl_3/AlEt_3$, heterogeneous Ziegler–Natta catalyst system.

As presumed by Blais and Manley[13], the changes of the polymerization conditions, such as types of catalyst systems (homogeneous and heterogeneous Ziegler–Natta, Phillips), the catalyst concentration, the reaction temperature and agitation, can have an influence on the morphology of the nascent polymers by affecting the polymerization rate. Although the main interest of the present work is not to establish polymerization kinetics, kinetic measurements were carried out in order to obtain a better understanding of the effect of the polymerization variables on the polymerization kinetics and furthermore to observe how these polymerization conditions change the morphology and macroconformation of the nascent polymer. A search of the literature on polymerization kinetics of ethylene, revealed that relatively little work has been published on experiments using a $TiCl_3$ catalyst for ethylene polymerization[18–22]. Many questions concerning this polymerization remain unsolved or are still open to discussion. On the contrary, polymerization kinetics of ethylene using Ziegler catalyst, based on $TiCl_4$ have been widely studied[23–26]. Kinetic studies are very useful in understanding the development of the polymerization with time and in obtaining data on the number of propagation centres. It is useful to know how these values change during polymerization, as it will help us to understand the crystallization process of the polymer during its growth on the catalyst surface. We have attempted in this paper to elucidate the conditions that control the polymerization rate. The polymerization reaction was carried out in a n-paraffin viscous medium, having in mind the ideas established by Wunderlich[10] on crystallization during polymerization. Due to the low solubility of the ethylene in this solvent, together with its high reactivity, it can

0032–3861/79/040474–09$02.00

Table 1 Kinematic viscosity of the paraffin solvent

Polymerization temperature (°C)	Viscosity (cps)
0	520.0
70	18.0
100	7.5
115	5.0
120	4.6

be expected at low stirring speed that polymerization occurs under conditions strongly controlled by mass transfer. Therefore, the polymerization rate could be reduced and brought near to the crystallization rate. At high stirring velocity, the polymerization reaction would be controlled chemically and the polymerization rate occurs so fast that polymerization and crystallization take place at very different times.

EXPERIMENTAL

Reagents

Careful precautions were taken to ensure anaerobic and anhydrous conditions for all polymerization experiments. Nitrogen was purified by passing it through different columns containing activated BASF R-3-11 catalysts in the reduced state, KOH Linde molecular sieve 4A, and $AlEt_3$ in n-heptane (1:1) in order to eliminate traces of oxygen, CO, CO_2 and water. Matheson polymerization grade ethylene (99.5% purity) was treated in the same way and was discharged from storage cylinder into the ethylene reservoir by cooling. Liquid n-paraffin was purified by treatment with a 10% solution of sodium permanganate in a water-acetone mixture; washed with distilled water and dried by storing over sodium wire. Finally LiH was added and the solvent distilled in a stream of nitrogen into a storage vessel immediately before use. The first 20% of the distillate was rejected and the fraction which distills between 40°–230°C and 10 mm Hg was collected. The paraffin was analysed by reaction with Br_2, HNa and infrared spectroscopy to make sure that unsaturated acid and alcohol groups were not present. The paraffin kinematic viscosities at different polymerization temperatures were determined by the method described in the ASTM 445-72 procedure and are given in *Table 1*. $TiCl_3$ grade AA purchased from Stauffer Chemical Co., also $AlEt_3$ from Ethyl Corporation, U.S.A., were used without further purification.

Polymerization technique and polymer characteristics

The polymerization procedure was carried out in the apparatus shown in *Figure 1*. Polymerizations were conducted in batch runs in a one-litre stirred glass autoclave, in order to observe the events occurring during the reaction. The temperature in the reactor was controlled to ±0.5°C by water pumped from a thermostat bath through the jacket. The runs were carried out at constant pressure in order to maintain constant ethylene concentration in the reaction system.

Both catalyst components were separately introduced into the reactor in a nitrogen stream. The experimental sequence was as follows: (a) The n-paraffin solvent was first added to the polymerization reactor from the storage burette. (b) the $TiCl_3$ solid components were then introduced in 300 cm^3 n-paraffin. (c) the required quantities of $AlEt_3$ co-catalysts were placed in a small container immediately above the solvent level. (d) the ethylene reservoir was placed on a weighing apparatus and connected to the reactor *via* a pressure reducing valve and a manometer. (e) the nitrogen was evacuated and ethylene admitted, with slow stirring of the solvent, to the required polymerization pressure. (f) by vigorously stirring, the $AlEt_3$ was released and quickly mixed. The stirring was set at the desired speed and the weight of the ethylene reservoir was measured during polymerization and the difference in weight recorded.

Withdrawal of samples during polymerization was effected by opening a valve fitted to the bottom of the reactor. The polymerizations were, in some cases, stopped by poisoning the catalyst with an excess of isopropanol. The decomposed polymer slurry was filtered when cold and added to a mixture of isopropanol containing 10% hydrocloric acid, and left for 24 h. The polymer was finally filtered, washed with isopropanol, water and acetone, then dried at 50°C under vacuum.

Intrinsic viscosities (corrected for non-Newtonian effects) of polyethylene samples were measured at 135°C in decalin[27]. The reproducibility of the $[\eta]$ values was better than 10%. The viscosity average molecular weights were calculated from intrinsic viscosities using the relationship[28].

$$|\eta| = 6.2 \times 10^{-4} \times \bar{M}_v^{0.70} \text{ (dl/gr)} \quad (1)$$

Electron microscopy

In order to observe the polymer growing on the catalyst surface, samples without catalyst decomposition were carefully deposited on SEM stubs and joined by a conductive-adhesive silver paint. The samples were then coated with gold under vacuum by a spattering technique to produce the necessary conducting surface. They were then examined at

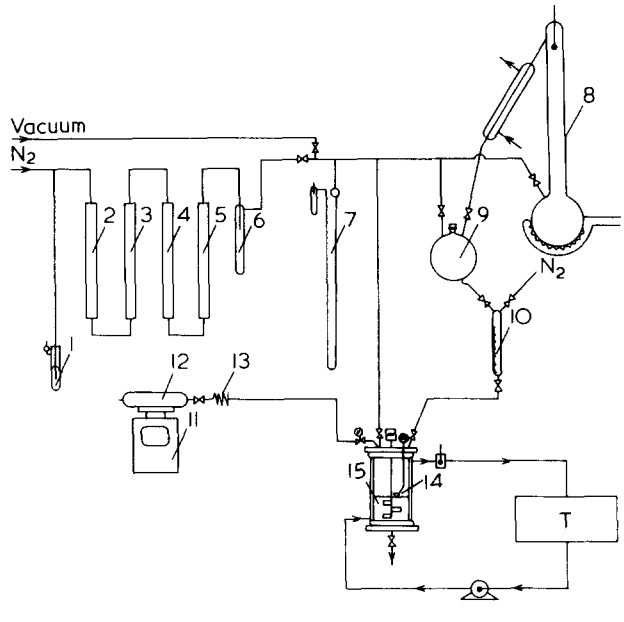

Figure 1 Polymerization systems. 1, Pressure relief valve. 2, R-3-11 BASF catalyst column. 3, KOH column. 4, Linde molecular sieve. 4a, Column. 5, $AlEt_3$ in heptane column. 6, Pressure relief vessels. 7, Manometer. 8, Solvent distiller. 9, Solvent storage vessels. 10, Storage burett. 11, Monomer weighting apparatus. 12, Ethylene reservoir. 13, Flexible connection. 14, $AlEt_3$ small container. 15, Polymerization glass autoclave. T, Thermostat baths

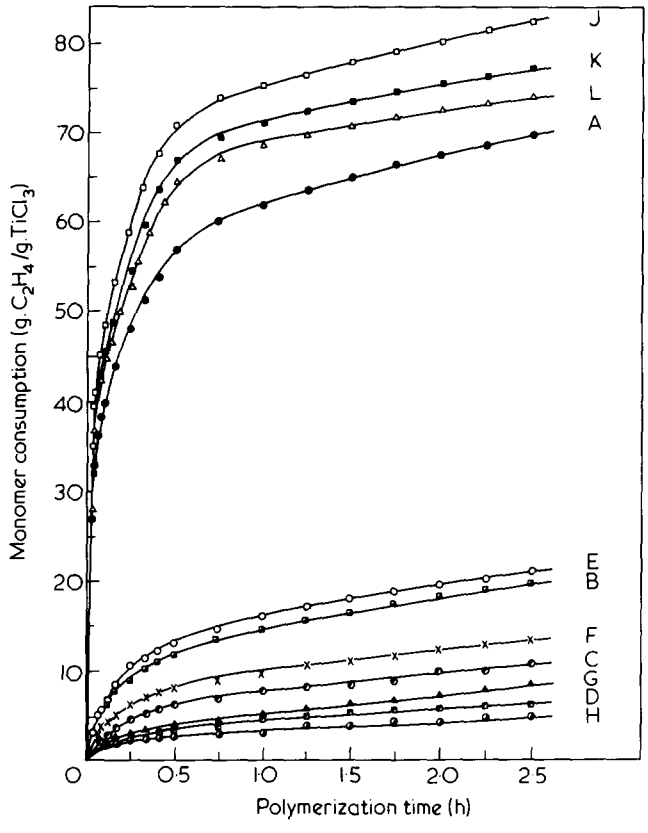

Figure 2 A, 10 atm., 70°C, 1000 rpm. B, 10 atm., 70°C, 10 rpm. C, 1 atm., 70°C, 1000 rpm. D, 1 atm, 70°C, 10 rpm. E, 10 atm., 0°C, 1000 rpm. F, 10 atm., 0°C, 10 rpm. G, 1 atm., 0°C, 1000 rpm. H, 1 atm., 0°C, 10 rpm. J, 10 atm., 100°C, 1000 rpm. K, 10 atm., 115°C, 1000 rpm. L, 10 atm., 120°C, 1000 rpm. [$TiCl_3$] = 11.6 mmol; molar ratio, $TiCl_3/AlEt_3$ = 1:5, Solvent paraffin 300 cm^3

20 kV with a scanning electron microscope (Cambridge Stereoscan). The electron beam was usually at 45° to the surface for maximum contrast.

RESULTS AND DISCUSSION

Polymerization rate

The amounts of ethylene per weight unit of $TiCl_3$ consumed at different polymerization conditions are given in *Figure 2*. The comparison between the various curves show the effect of the reaction variable such as temperature, pressure and stirring on the polymerization. The polymerization starts quickly at the beginning of the reaction for high temperature (70°C), pressure (10 atm) and agitation (1000 rpm) values (see curve A). This is due to the fact that the highest solubility of the monomer in the reaction medium was obtained under these conditions. Drastic reduction of these variables also decreased the amount of ethylene reacted e.g. comparison of curve A with curve B shows the effect of reducing the stirring speed from 1000 to 10 rpm. At low stirring speed the polymerization rate is strongly controlled by mass transfer. On the other hand, if the values for any one variable are low, changes in the others does not greatly affect the polymerization rate. For instance, comparing curves E with F – both a low temperature (0°C) – it can be observed that changes in the stirring speed are not very marked.

The polymerization rates obtained from the slopes of the curves in *Figure 2*, are given in *Figure 3*. It can be seen that for all polymerization conditions the kinetic curves are of the so-called 'decay' type, as reported in the literature using $AlEt_3$ as co-catalyst[20]. This includes also those reactions which are strongly controlled by the mass transfer of

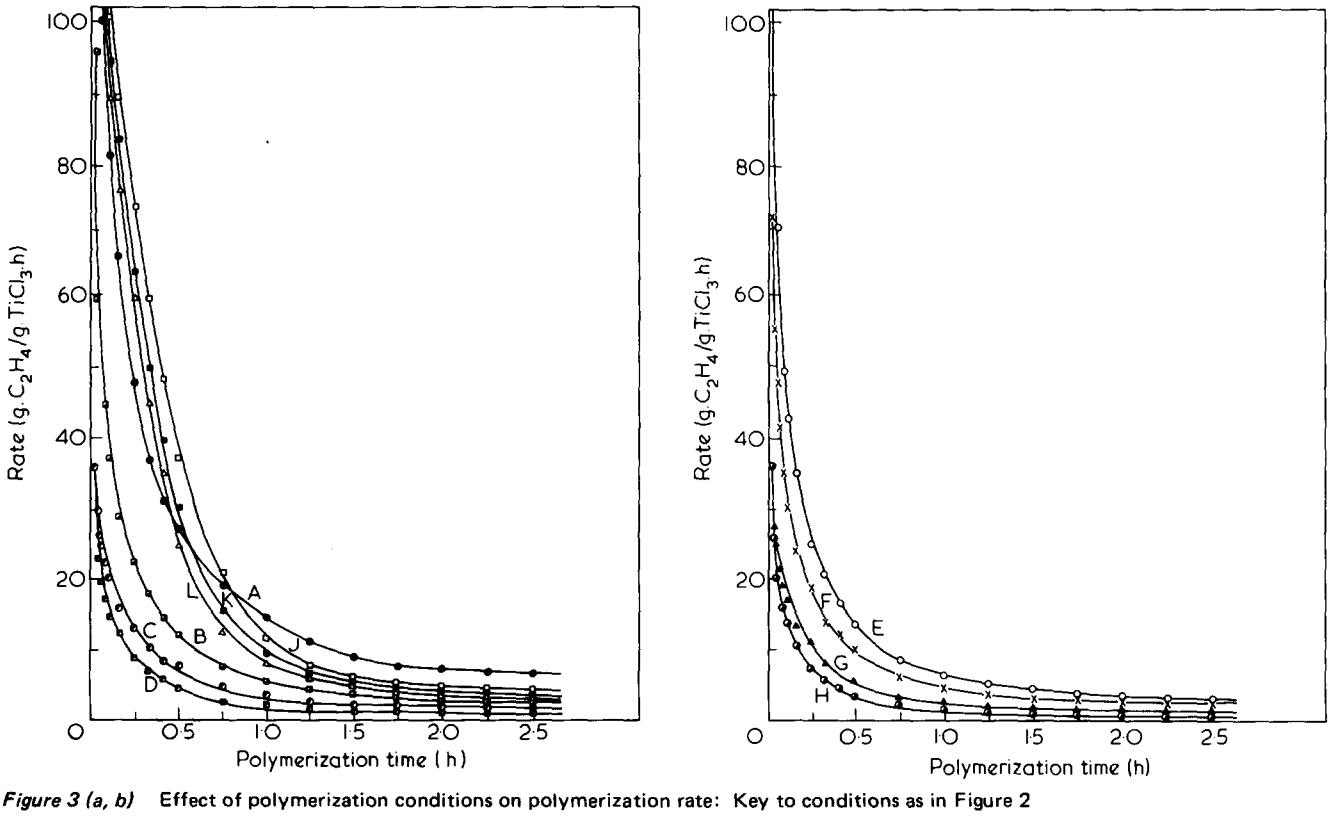

Figure 3 (a, b) Effect of polymerization conditions on polymerization rate: Key to conditions as in Figure 2

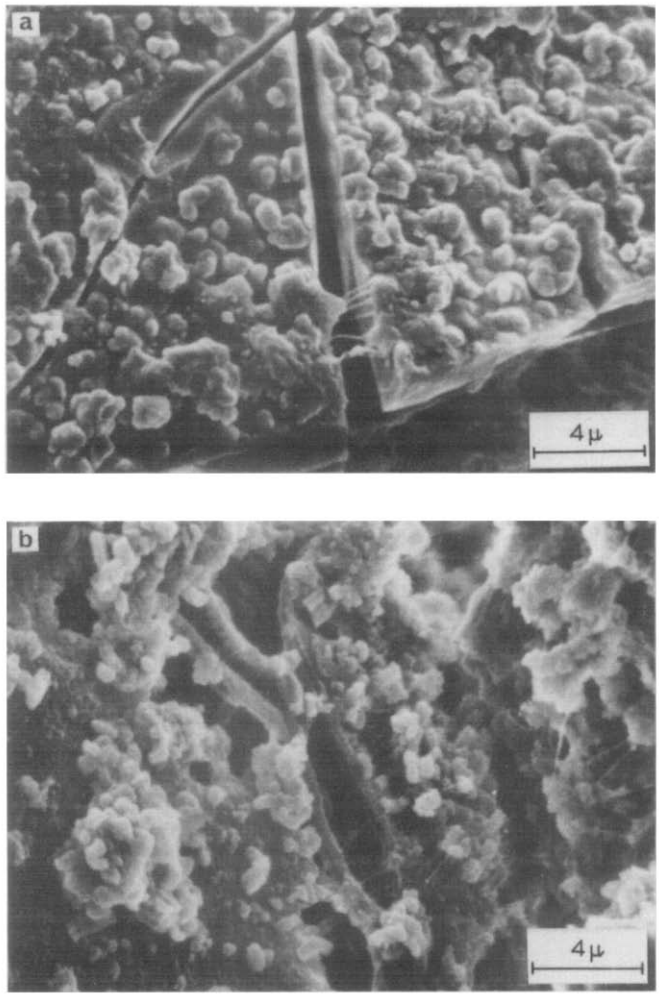

Figure 4 Cracks formation on the surface of $TiCl_3$ aggregates: without (a) and with (b) polymer growth on the freshly formed crystal edge by cleavage. Number of observed globules is about 10^8 cm^{-2}

the monomer. However, employing $AlEt_2Cl$, 'acceleration' type kinetic curves have been found[20]. The build-up period during which the polymerization rates increase rapidly to a maximum (R_0), cannot be observed by using very fine $TiCl_3$ such as AA-grade commercial catalyst from Stauffer Chemical Co., or by grinding H-$TiCl_3$ and A-$TiCl_3$ grade catalyst[29]. In such cases only the decay period during which the rate decreased gradually to the stationary state (R_∞) was observed. For the polymerization of propylene using the same catalyst system, the build-up period was observable, due to the lower reactivity of this monomer. With high activity supported Ziegler–Natta catalyst, on the other hand, only the decay period can be seen[30]. In general, the ethylene and propylene kinetic behaviour is similar and therefore the same equations can be applied.

The build-up period has been explained by a number of workers on the assumption that crystals and aggregates of $TiCl_3$ are broken and ground under the mechanical action of the growing polymer chains and also by local heating due to the exothermal polymerization reaction. Therefore the number of active sites on the crystal edges would increase because of the newly formed surfaces[13,30]. This effect can be observed by using SEM techniques as can be seen from the photographs in *Figure 4*, taken at the earliest stages of the polymerization and under reaction conditions which correspond to a slow polymerization rate (e.g. low stirring or temperature). The average size of globules growing on the catalyst surface was of the order of 10^8 cm^{-2}. Furthermore, deposition of a polymer layer on the catalyst surface can be seen as the polymerization continues. At high polymer yield encapsulation of catalyst particles by the polymer occurs[31–33]. Finally, it was possible to find newly growing polymer molecules within some of the already formed polymer masses as can be seen in *Figure 5*, indicating that either all polymer chains do not start to grow at the beginning of the reaction, but that new growths occur during the polymerization, or that there are polymerization loci with different activities, as can be seen in *Figure 5*.

The decay period has been defined by the following equations[20]:

$$\frac{dR}{dt} = k_3(R - R_\infty) \tag{2}$$

or

$$\frac{R - R_\infty}{R_0 - R} = \exp(-k_3 t) \tag{3}$$

where the constant k_3 can be considered as the constant of the first order rate low governing the approach of R to R_∞.

The validity of the mathematical equation (3) for different polymerization temperatures is shown in *Figure 6*.

Two different explanations are given for the decrease in the polymerization rate during the decay period. One of them is based predominantly on chemical reasoning, involving destruction or chemical deactivation of one type of active centre to give a constant concentration in the steady state[24,34,35], or alternatively, the supposition of two types of active sites, time-deactivation occurring to one of them[36]. The other interpretation is based on a physical effect, such as agglomeration of $TiCl_3$ particles by mechanical action of the polymer formed during the reaction[29] and also by embedding of the catalyst particles within the polymer mass forming a cluster, which prevents or hinders the mass transfer of the monomer through the polymer layer, to the growth sites[37,38].

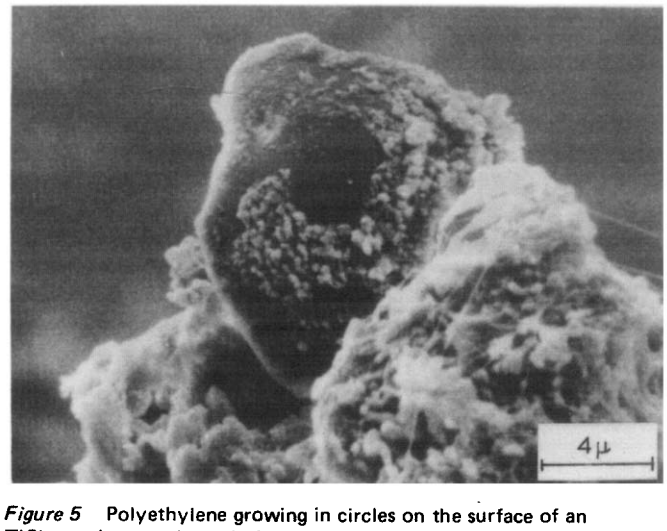

Figure 5 Polyethylene growing in circles on the surface of an $TiCl_3$ catalyst particle within the polymer mass

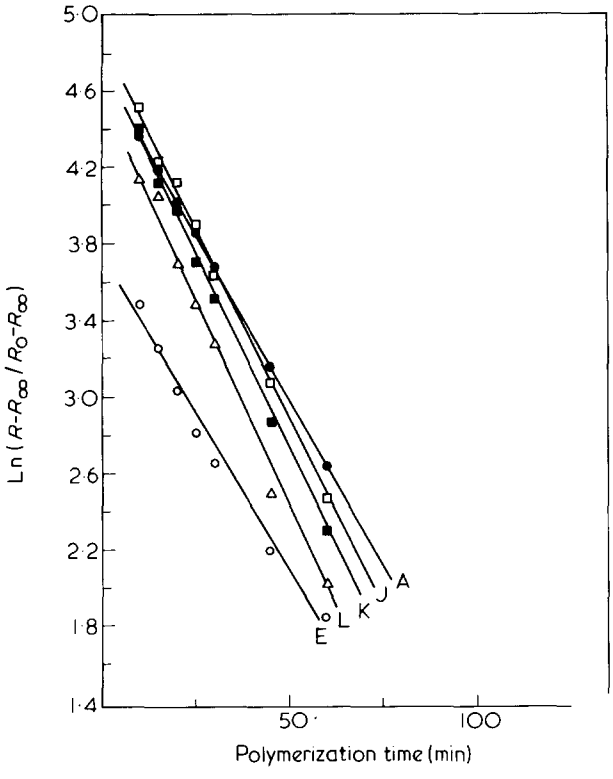

Figure 6 Kinetic data according to equation (3) for ethylene polymerization with $TiCl_3/AlEt_3$ catalyst system and different polymerization conditions. Key as in Figure 2

Temperature effect on polymerization rates

The rate increases as the temperature rises to 100°C and falls off rapidly as the temperature continues increasing (see curves J, K and L in *Figure 3(a)*. This is due, as established by Berger and Grieveson[18], to a decrease of the solubility of the monomer in the solvent by raising the temperature. The solution rate of the ethylene in the solvent is too low to satisfy the potential polymerization activity of the catalyst. In spite of this, sometimes only chemical interpretations such as deactivation of the active centres at high temperature have been given to explain this phenomenon[26,38–40]. However, as it can be seen later, the number of growing chains always increases with the temperature, as has also been found by Zakharov *et al.*[41]. Based on these new results we believe that the deceleration of the polymerization rate at high temperatures is possibly due to the overall mass transfer of the monomer to the catalyst surface where the active centres are located together with a change of the active centre types by chemical reaction[41].

The overall activation energies for the maximum of the build-up period and the decay and stationary periods can be obtained from Arrhenius plots.

The maximum polymerization rate R_0 is given by the following equation:

$$R_0 = k_2 P |A| t \qquad (4)$$

where P is the ethylene pressure, $|A|$ is the concentration of the organometallic compound, t is the polymerization time and k_2 is a constant. The activation energy obtained by plot of $R_0/P|A|t$ against $1/T$, as shown in *Figure 7* was 8.4 kcal/mol (corrected by taking into account the heat of solution 3.0 kcal/mol of ethylene).

In spite of the fact that the stationary period depends on co-catalyst concentration as established by Schnecko *et al.*[42], Keii[20], Schindler[43], and other workers, Natta's rate law can be used to obtain the overall activation energy. This is justifiable since we work at constant $AlEt_3$ concentration. The stationary polymerization rate could be expressed in the following form[29]:

$$R_\infty = kGP \qquad (5)$$

where G is the mass of $TiCl_3$. The corrected activation energy obtained by plot of R_∞/GP against $1/T$ (0° to 70°C) (*Figure 7*) was 5.0 kcal/mol. The values found in each case are broadly in agreement with those reported in the literature for Ziegler–Natta type polymerizations of ethylene, (*Table 2*), with the exception of that reported by Berger and Grieveson[18]. The overall activation energy for the decay period obtained from the plot of k_3 *versus* $1/T$ (*Figure 8*) was about 3.5 kcal/mol. This result is similar to those reported by Keii[20,32], for ethylene (4.8 kcal/mol) and propylene (2 ~ 3 kcal/mol) polymerization.

The nature of the decay process is not clear at present. However, Keii suggests that the most plausible mechanism is that of deactivation of the surfaces sites due to structural changes in $TiCl_3$ crystals, such as migration of Cl^- from an adjacent lattice to a surface defect as postulated in Cossee's model[20]. The activation energy for this process was established in the range of 2 ~ 3 kcal/mol. This could be questioned because the same kinetic relationships are approximately obeyed by those polymerization conditions controlled by mass transfer process.

Factors controlling molecular weight and number of growing chains

Samples were taken out from the reactor during polymerization in order to study the growth of the polymer chains

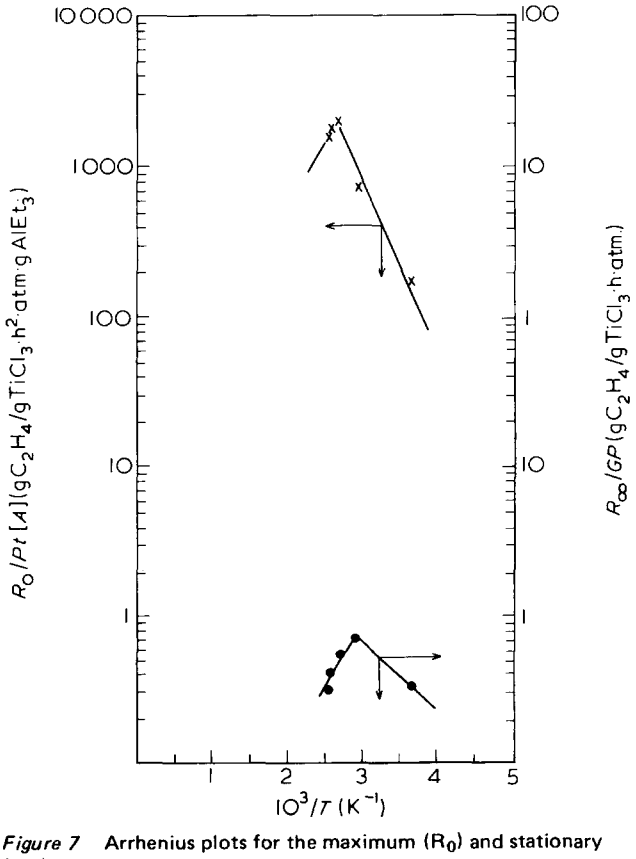

Figure 7 Arrhenius plots for the maximum (R_0) and stationary (R_∞) polymerization rate

Table 2 Activation energy of ethylene polymerization

Catalyst system	A/Ti	Temperature range (°C)	Activation energy (kcal/mol)	References
$AlEt_3/TiCl_3$	4:1	10– 60	9.7	(45)
$AlEt_3/TiCl_3$	5:1	0–100	8.4	This work (R_0)
$AlEt_3/TiCl_3$	5:1	0– 70	5.0	This work (R_∞)
$AlEt_3/TiCl_3$	1:1	20– 80	5.9	(41)[b]
$AlEt_3/TiCl_3$	6.6:1	0–100	7.8	(26)
$AlEt_3/TiCl_3$	2:1	–	7.3	(44)
$AlEt_3/TiCl_3$	10.7:1	–	8.4	(44)
$AlEt_3/TiCl_3$	1:1	0– 50	17.3	(18)
$AlEt_3/TiCl_4$	6.6:1	0– 85	2.7	(26)
$AlEt_3/TiCl_4$	1.7:1	−1 to −56	6.2	(25)
$AlEt_2Cl/TiCl_3$	6:1	10– 60	8.9	(45)
$AlEt_2Cl/TiCl_3$	1:1	0– 90	7.0	(46)
$AlEt_2Cl/TiCl_3$	1:0	–	7.5	(44)
$AlEt_2Cl/TiCl_3$	2:0	–	8.4	(44)
$AlEt_2Cl/TiCl_3$	5:5	–	8.2	(44)
$AlEt_2Cl/TiCl_3$	10.0:1	–	8.0	(44)

[a] In SI-units 1 cal = 4.184 J
[b] Value obtained also from R_∞

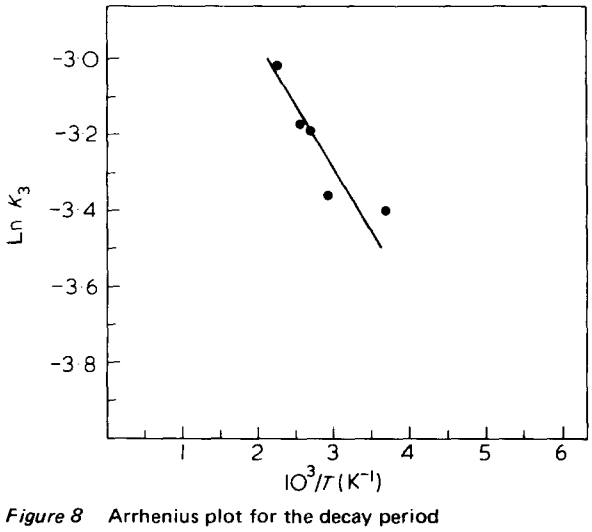

Figure 8 Arrhenius plot for the decay period

and *Figure 9* shows the change of the molecular weight for different polymerization conditions. During the initial stages the molecular weight increases with time, followed by a long slow asymptotic increase. By comparing curve A with curves B, C and E, the effects of the variables such as stirring, pressure and temperature, on the molecular weight are apparent. Furthermore, by comparing curves E and F, the effects of stirring at low polymerization temperature, can also be observed. It can be concluded that the polymerization temperature is the more important factor controlling the molecular weight and that the effect of the other variables is more marked at low polymerization temperatures.

The molecular weight decreases nearly exponentially with temperature rise, and the plot of log M.Wt. vs $1/T$ gives straight lines for different polymerization times (*Figure 10*). In addition, the molecular weight continuously increases with the polymer yield, (*Figure 11*) due to the fact that the polymerization rate is always 3 orders of magnitude larger than the rate of the chain transfer reactions[21].

Finally, measurements of the polymerization rate and molecular weight enable us to evaluate the number of polymer chains. As established experimentally by Keii[20] the dependence of molecular weight on polymerization time during the decay period can be represented by

$$\frac{I}{\bar{M}_v} = \frac{I}{\bar{M}_\infty} + \frac{\beta}{t} \qquad (6)$$

where $\bar{M}_v$ is the viscosity average molecular weight, $\bar{M}_\infty$ is the limiting value for infinite polymerization time and β is a coefficient.

Figure 12 shows the validity of the equation (6) for different polymerization conditions, and permits the calculation of $\bar{M}_\infty$, (*Table 3*).

The number-average-molecular weight at a given time t is:

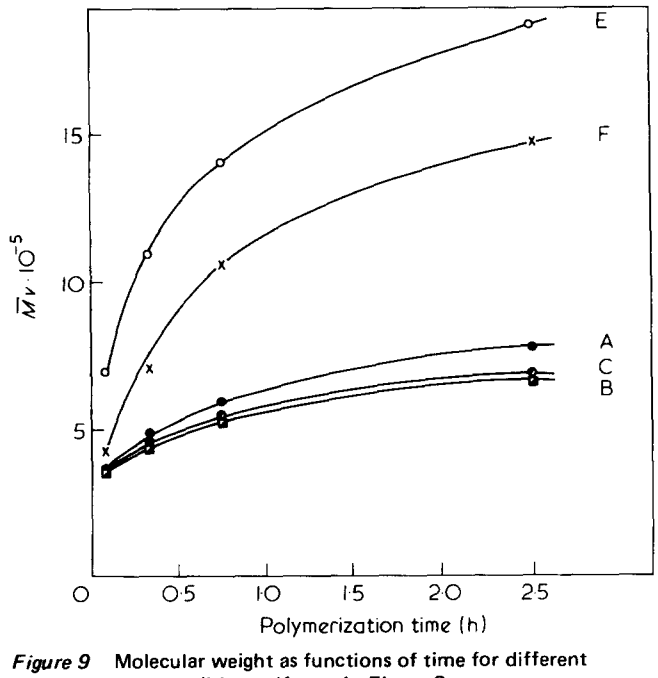

Figure 9 Molecular weight as functions of time for different polymerization conditions. Key as in Figure 2

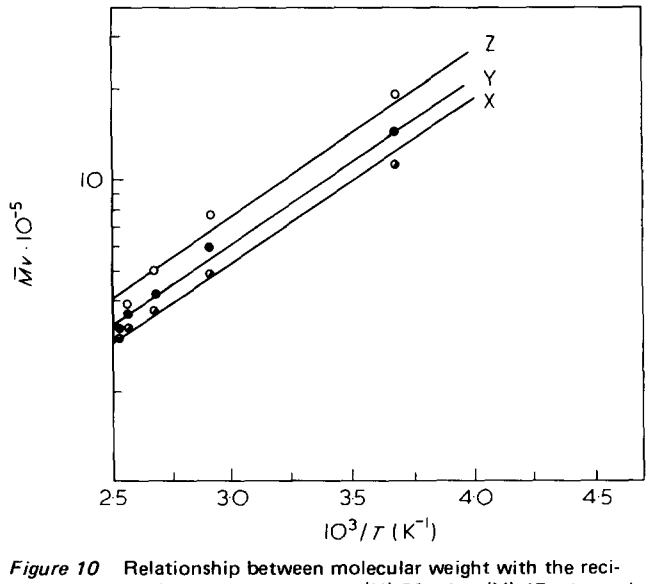

Figure 10 Relationship between molecular weight with the reciprocals polymerization temperature: (X) 20 min. (Y) 45 min. and (Z) 150 min. polymerization time

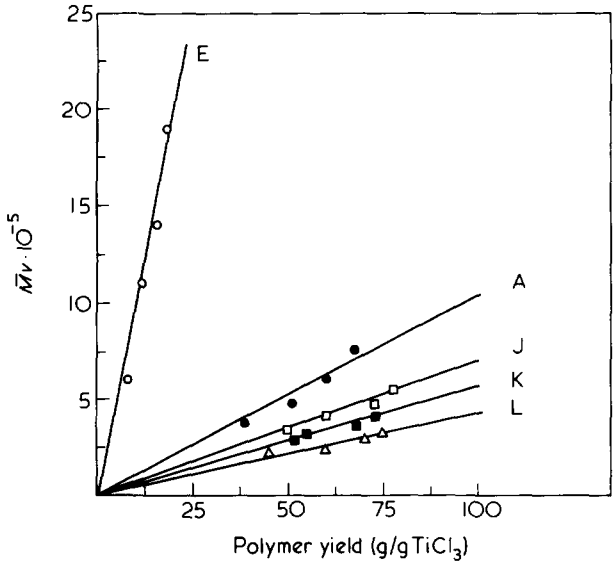

Figure 11 Dependence of molecular weight with polymer yield at different polymerization temperature. Key as in Figure 2

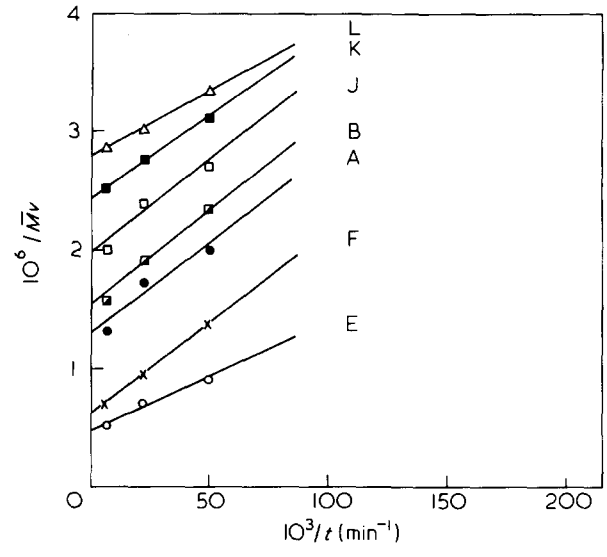

Figure 12 Kinetic data according to equation (6) for ethylene polymerization with $TiCl_3/AlEt_3$ catalyst system and different polymerization conditions. Key as in Figure 2

Table 3 Intrinsic viscosity, average molecular weight, concentration and number of growing polymer chain in the ethylene polymerization with $TiCl_3/AlEt_3$. [$TiCl_3$] = 11.6 mmol, molar ratio $TiCl_3/AlEt\ell$ = 1:5., solvent paraffin = 300 cm^3

Run[a] Nr.	Polymerization time (min)	(dl/gr)	Molecular weight $\bar{M}_v \times 10^{-4}$	Molecular weight $\bar{M}_\infty \times 10^{-4}$	$\int_0^t Rdt$ / (g.C_2H_4/g.$TiCl_3$)	Concentration of growing Poly. chain (mol/l) 10^{-5}	Number of growing Pol. chain $10^{-13}/cm^2$
A	5	4.80	36.6	80.0	43.8	37.6	18.6
	20	5.90	48.5		53.7	57.8	27.8
	45	6.80	60.0		59.8	14.3	7.0
B	5	4.70	35.0	70.0	6.8	5.7	2.8
	20	5.40	43.0		11.0	5.7	2.8
	45	6.20	52.0		13.3	3.9	1.8
C	5	4.70	35.0	70.5	3.7	3.2	1.5
	20	5.50	44.0		5.6	2.8	1.3
	45	6.30	54.0		6.5	1.7	1.0
E	5	7.60	69.3	221.0	8.0	4.7	2.3
	20	10.50	110.8		12.2	3.3	1.6
	45	12.50	142.6		14.9	2.2	1.1
	150	15.30	190.4		21.2	0.9	0.4
F	5	5.40	43.0		5.3	5.4	2.5
	20	7.80	72.0	162.0	7.4	3.4	1.6
	45	10.10	106.0		8.75	1.7	0.8
	150	12.80	146.0		12.5	0.5	0.2
J	5	4.50	33.4	81.0	53.7	43.4	20.8
	20	5.20	41.0		67.5	–	–
	45	5.80	48.0		74.0	19.6	9.4
	150	6.50	56.0		82.5	7.2	3.4
K	5	4.20	29.7	44.0	48.7	31.8	15.3
	20	4.40	32.0		63.6	32.4	15.5
	45	4.90	37.0		69.0	17.7	8.5
	150	5.30	41.4		77.2	6.6	3.2
L	5	3.30	21.5	35.0	47.5	50.8	24.4
	20	3.60	23.8		61.0	48.9	23.5
	45	4.10	29.2		67.0	22.6	10.8
	150	4.40	31.7		73.75	13.1	6.3

[a] A, 10 atm., 70° C, 1000 rpm; B, 10 atm., 70° C, 10 rpm; C, 1 atm., 70° C, 1000 rpm; E, 10 atm., 0° C, 1000 rpm; F, 10 atm., 0° C, 10 rpm; J, 10 atm., 100° C, 1000 rpm; K, 10 atm., 115° C, 1000 rpm; L, 10 atm., 120° C, 1000 rpm

$$\bar{M}_n = \frac{\text{weight of monomer consumed at time } t}{\text{no. of polymer molecules produced at time } t}$$

$$= \frac{\int_0^t Rdt}{[C^*]_t + \int_0^t \sum R_t dt} \quad (7)$$

where

$\int_0^t Rdt$ is the g. of monomer consumed up to time t,

$[C^*]$ number of growing polymer chains

$\int_0^t R_t dt$

number of polymer chains completed up to time t.

Assuming that all chains grow to $\bar{M}_\infty$ or $R/\Sigma R_t$ = const = $\bar{M}_\infty$ it is obtained:

$$\frac{1}{\bar{M}_n} = \frac{[C^*]_t}{\int_0^t Rdt} + \frac{1}{\bar{M}_\infty} \quad (8)$$

and

$$[C^*]_t = \left\{\frac{1}{\bar{M}_n} - \frac{1}{\bar{M}_\infty}\right\} \int_0^t Rdt \quad (9)$$

The number of growing polymer chains calculated from (9) are given in *Table 3*.

Assuming a specific surface area of 21 m^2/g. for the AA-grade $TiCl_3$[20,41,47] the number of growing chains per unit surface area can also be obtained (*Table 3*). These values are in close agreement with those obtained by other methods reported in the literature. Schnecko *et al.*[21] have reported values ranging between $5.1 \sim 7.6 \times 10^{-5}$ mol/l for the $TiCl_3/AlEt_2Cl$ system, determined by quenching the polymerization with tritiated butanol. Zakharov *et al.*[41] found values of $2 \sim 6 \times 10^{-5}$ mol/l at 75°C for the δ-$TiCl_3/AlEt_3$ system, terminated by quenching the polymerization with radioactive carbon monoxide. On the other hand, our values range between $0.5 \sim 57 \times 10^{-5}$ mol/l, depending on the polymerization temperature. The number of growing polymer chains per unit surface are in the range of $27 \sim 0.2 \times 10^{13}$ cm^{-2} and are close to the value of 11.2×10^{13} cm^{-2} found by Keii[20]. As will be shown in part III[33] the concentration of growing polymer chains on the catalyst surface is a very important factor controlling the as-polymerized morphology of the polyethylene. For low concentration of growing polymer chains (low polymerization temperature) a globular morphology was obtained, while at high concentration a wormlike morphology originates.

REFERENCES

1 Geil, P. H. 'Polymer Single Crystals', John Wiley (Interscience) New York, 1963
2 Keller, A 'Polymer Crystals' in *Rep. Prog. Phys.* 1968, **31**, 623
3 Wunderlich, B. 'Macromolecular Physics' **I**, Academic Press Inc., New York, 1974
4 Fava, R. A., Polyethylene crystals, *J. Macromol. Sci. Rev. Macromol. Chem.* 1971, **5**, I, 1975
5 Blackadder, D. A. *J. Macromol. Sci. Rev. Macromol. Chem.* 1967, **C I(2)**, 297
6 Stuart, H. A. 'Die Physik der Hochpolymeren' **4**, Springer Verlag, Berlin, 1956
7 Schultz, J. M., 'Polymer Material Science', Prentice Hall, Inc. New Jersey 1974
8 Wunderlich, B. 'Macromolecular Physics' **2**, Academic Press, Inc. New York, 1977
9 Wegner, G., Fischer, E. W., Muñoz-Escalona, A. *Makromol. Chem. Supp.* 1975, **I**, 521
10 Wunderlich, B. *Adv. Polym. Sci.* 1968, **5**, 568
Wunderlich, B. *Angew. Chem. Int. Ed. Engl.* 1968, **7**, 912
11 Herman, D. F., Kruse, U. Broncato, J. J. *J. Polym. Sci. (C)* 1965, **II**, 75
12 Chanzy, H. D., Coté, W. A., Marchessault, R. H. *Textile Res. J.* 1969, **38**, 581
13 Blais, P., Manley, R. J. St., *J. Polym. Sci. (A-1)*, 1968, **6**, 291
14 Ingram, P., Schindler, A. *Makromol. Chem.* 1968, **III**, 267
15 Keller, A., Willmouth, F. *Makromol. Chem.* 1969, **121**, 42
16 Marchessault, R. H., Chanzy, H. D. *J. Polym. Sci. (C)*, 1970, **30**, 311
17 Muñoz-Escalona, A., Guerrero, S. J. *Makromol. Chem.* 1976, **177**, 2149, 2160
18 Berger, M. N., Grieveson, B. M. *Makromol. Chem.* 1965, **84**, 80
19 Grieveson, B. M. *Makromol. Chem.* 1965, **84**, 93
20 Keii, T., 'Kinetics of Ziegler–Natta Polymerization', Chapman and Hall, London, 1972
21 Schnecko, H., Jung, K. A., Kern, W. in 'Coordination Polymerization', Ed. J. C. W. Chien, Academic Press, Inc., New York, 1975, p 73
22 Fuji, S. in 'Coordination Polymerization', Ed. J. C. W. Chien, Academic Press, Inc., New York, 1975, p 135
23 Schindler, A. *J. Polym. Sci. (C)* 1963, **4**, 81
24 De Vries, Hn., *Rec. Trav. Chim.* 1961, **80**, 866
25 Meshkova, I. N., Bakova, G. M., Tsvetkova, V. I., Chirkov, N. M. *Polym. Sci. U.S.S.R.* 1961, 1011
26 Fukai, R., Kagiya, T., Machi, S., Shineidzu, T., Yuasa, S. *Bull. Chem. Soc. Jpn*, 1962, **35**, 303, 306
27 Tung, L. H. *J. Polym. Sci.* 1957, **24**, 333
28 Chiang, R. *J. Phys. Chem.* 1965, **69**, 1945
29 Natta, G., Pasquon, I. *Adva. Catalysis* 1959, **II**, I
30 Muñoz-Escalona, A., Villalba, J. *Polymer*, 1977, **18**, 179
31 Corradini, W. R. Jr., Rase, W. F. *J. Appl. Polym. Sci.* 1971, **15**, 889
32 Keii, T., Soga, K., Saiki, N. *J. Appl. Polym. Sci.* 1967, **16**, 1507
33 Muñoz-Escalona, A., Parada, A. to be published in this Journal
34 Ambroz, J., Osecky, P., Mejzlik, J., Hamerick, O. *J. Polym. Sci. (C.)* 1967, **16**, 423
35 Kohn, E., Shuurmans, H. J. L., Cavender, J. V., Mendelson, R. M. *J, Polym. Sci.* 1962, **58**, 681
36 Keii, T., Soga, K., Go, S., Takahashi, A., Kohima, A. *J. Polym. Sci. (C)* 1968, **23**, 453
37 Pasquon, I., Dente, M., Marduzzi, F. *Chim. Ind. (Milan)* 1959, **41**, 387
38 Allen, P. E., Gill, D., Patrick, C. R. *J. Polym. Sci. (C)* 1964, **4**, 127
39 Natta, G., Mazzanti, G., De Lucca, D., Giannini, U., BAndini, F. *Makromol. Chem.* 1964, **83**, 54
40 Kodama, S., Kagiya, T., Machi, S., Shimidzu, T., Yuasa, S. Fukui, K. *J. Appl. Polym. Sci.* 1960, **7**, 20

41 Zakharov, V. A., Chumaesvskii, Bukatov, G. D., Yermakov, Y. I. *Makromol. Chem.* 1976, **177**, 763
42 Schnecko, H., Reinmoller, M., Weirauch, K., Kern, W. *J. Polym. Sci. (C.)* 1963, **4**, 71
43 Schindler, A. *J. Polym. Sci. (C)* 1964, **4**, 81
44 Lanovskaya, L. M., Makletsova, N. V., Gautmakher, A. R. Medvedev, S. S., *Vysokomolekul. Soedin* 1965, **7**, 741, 747 quoted by Keii, T., in 'Kinetics of Ziegler–Natta Polymerization', Chapman and Hall, London, 1972, p 160
45 Belov, G. P., Bogomolova, N. B., Tavetkova, V. I., Chirkov, N. M. *Kinetika i Kataliz*, 1966, **8**, 229
46 Matsuda, T., Keii, T., Kojima, A., Ishida, T. *Kogya Kagaku Zasshi*, 1968, **71**, 1124, 1128 quoted by Keii, T., in 'Kinetics of Ziegler–Natta Polymerization', Chapman and Hall, London, 1972, p 160
47 Schnecko, H., Dost, W., Kern, W. *Makromol. Chem.* 1969, **121**, 159